

Thermal conductivity and electrical resistivity of copper in intense magnetic fields at low temperatures

R. W. Arenz, C. F. Clark, and W. N. Lawless

CeramPhysics, Inc., Westerville, Ohio 43081

(Received 1 March 1982)

Measurements are reported for the first time of a complete set of thermal conductivity and electrical resistivity data, both transverse and longitudinal, in fields up to 12.5 T between 3 and 15 K for a polycrystalline sample of copper (residual resistivity ratio equal to 108). The transverse resistivity data obey the Kohler rule at all field levels; the longitudinal data, only at higher fields ($H \geq 5$ T). The longitudinal resistivity data do not show saturation. The transverse thermal conductivity is depressed more by intense fields than is the longitudinal conductivity. Effective Lorentz numbers, defined by the Wiedemann-Franz law, are determined: The longitudinal Lorentz number is H -field independent, but the transverse Lorentz number is found to increase linearly with H . The latter dependence is significant, $dL/dH = 0.112 \times 10^{-8}$ W Ω K $^{-2}$ per tesla.

INTRODUCTION

Electron transport in metals has occupied a central role in physics for a long time, particularly as one of the early successes of quantum physics. The Wiedemann-Franz law relates the thermal conductivity K to the electrical resistivity ρ ,¹

$$K\rho/T = L = (\pi k/e)^2/3, \quad (1)$$

where L is the Lorentz number and T is the absolute temperature. The derivation of Eq. (1) does not depend on any assumptions about the details of the Fermi surface and is valid for all metals. This law is a good approximation for most metals² due to a fortuitous cancellation of the electron mean free path at the edge of the Fermi surface in the derivation.³ At low temperatures the Wiedemann-Franz law is valid provided that (1) the phonon contribution to the thermal conductivity is negligible, and (2) the conduction electrons are scattered elastically. The latter condition requires that the temperature-independent, electron-impurity scattering dominates over the electron-phonon scattering.

Electron transport in magnetic fields is usually represented by Kohler's rule⁴ in the form of a universal function,

$$\Delta\rho/\rho_0 = f(H/\rho_0), \quad (2)$$

where $\Delta\rho$ is the change in resistivity in field H . Experimentally, Kohler's rule is strictly obeyed only when electron scattering by nonmagnetic impurities is dominant.⁵ Copper and gold follow Eq. (2) at low temperatures for fields up to 10 T, but

aluminum and indium show significant deviations from Kohler's rule.⁶

In the present investigations, we have measured the electrical resistivity *and* thermal conductivity of a copper wire which satisfies the validity conditions for the Wiedemann-Franz and Kohler laws. Measurements were made in both transverse *and* longitudinal magnetic fields up to 12.5 T at temperatures between 3–15 K. We believe that these measurements represent the first *complete* data set measured on the *same* sample of copper, and the goal here is to examine both the validity and anisotropy of Eqs. (1) and (2) in intense magnetic fields.

Our original purpose for pursuing these measurements was related to the development of a method for measuring specific heats in intense fields at low temperatures using a variation of the "calibrated wire" technique.⁷ In this case the calibrated wire is the copper wire reported here, and the calibration required measuring the transverse and longitudinal thermal conductivity in intense fields.

EXPERIMENTAL METHOD AND RESULTS

The copper wire was from a commercial spool and had a diameter of 0.079 mm and a residual resistivity ratio (RRR) of 108. The resistance of a section of this wire in zero field between 1.5–25 K is shown in the inset of Fig. 1. The resistance, and hence the resistivity, is essentially temperature-independent below ~ 15 K, and hence the electron scattering is dominated by impurities rath-

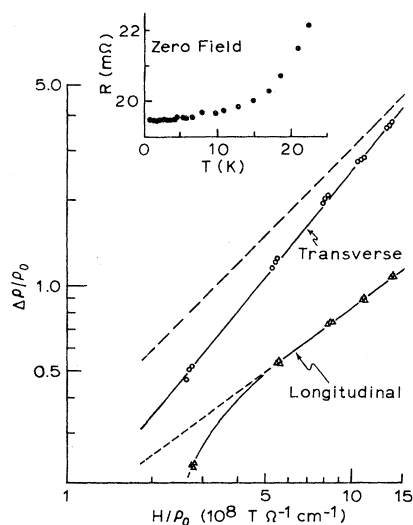


FIG. 1. Kohler plots of the transverse and longitudinal magnetoresistance of the copper wire measured. The data points shown are for 3, 7, and 10 K. The dashed curve is the Kohler fit obtained by Fickett (Ref. 5) from the magnetoresistance of a large number of copper samples. The inset shows the resistance of the wire, 1.5–25 K, in zero field measured on a separate sample.

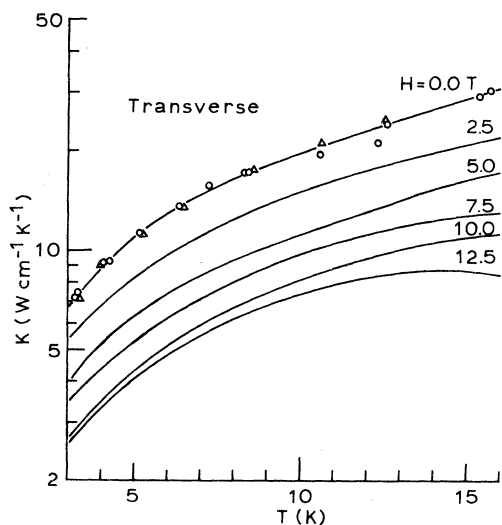


FIG. 2. Transverse magnetothermal conductivity data for the copper wire. At zero field, measured data are shown for both the transverse sample (triangles) and the longitudinal sample (circles). The curve through the zero-field data is the third-order fit discussed in the text. The curves for $H > 0$ were obtained by the procedure described in the text for separating the transverse and longitudinal components.

er than by phonons, thus satisfying the electron scattering condition mentioned above.

The phonon contribution to the thermal conductivity at low temperatures is given by⁸

$$K_l \cong (310K_\infty / GN^2\Theta_D^2)T^2, \quad (3)$$

where K_∞ is the conductivity at high temperatures, G is a constant $\cong 70$, N is the number of free electrons per atom, and Θ_D is the Debye temperature. For copper ($N = 1$, $\Theta_D = 313$ K), $K_l \cong 1.8 \times 10^{-4} T^2$ ($\text{W cm}^{-1} \text{K}^{-1}$), which is negligibly small for the copper wire used here even at 12.5 T (e.g., see Fig. 2). Consequently, the copper studied here satisfies the validity conditions for the Wiedemann-Franz and Kohler relations.

The magnetic field measurements were made in a 14-T superconducting magnet. The sample holder consisted of a brass can which fitted into the tailpiece of the insert Dewar of the magnet, and the can was suspended on a long, stainless-steel tube which served as both the pumping line and the conduit for electrical leads. Attached to the flange of the brass can was a copper post on which the samples were mounted. This copper post was attached to the flange with a stainless-steel link designed so that the post could be temperature-controlled without a large loss of liquid helium. Heater leads were wrapped at the top of the copper post and were powered by a commercial temperature controller which operated from a silicon diode mounted in the post. Also mounted within the post was a calibrated germanium thermometer which was used to calibrate the capacitance thermometer⁹ mounted on the sample in zero field at the start of each run (see below). For controlling temperatures in magnetic fields, the calibrated capacitance thermometer was used to determine the set point of the controller.

The electrical leads were heat sunk both at the flange of the brass can and at the top of the copper post. Radiation baffles were placed in the stainless-steel tube, and zeolites were placed in the bottom of the can. The sample holder was evacuated at room temperature before cooldown, and no helium exchange gas was used. The cooldown time for the copper post was ~ 3 h to reach helium temperatures, and it was found that this cooldown time was sufficient to stabilize the capacitance thermometers against drifting.¹⁰ The brass can was lined with aluminized Mylar, and the estimated radiation-transfer heat load on the samples was $< 1 \mu\text{W}$ under worst conditions (sample at 15 K, can at 1.5 K). This radiation load was negligible;

in the thermal conductivity measurements, for example, typical heater powers were ≥ 1 mW.

In all the measurements here, the capacitance thermometers were calibrated in zero field at 6–8 points between 3–15 K, and the $C - T$ data were fitted to a fourth-order expansion.¹¹ The uncertainty in the measurements of absolute temperatures from this procedure is $\lesssim 15$ mK. The samples were placed in the homogeneous field region of the magnet, and based on the magnet specifications we estimate that the uncertainty in the field measurements is $\lesssim 0.05$ T. The capacitance thermometers were measured using a transformer-ratio-arm bridge plus oscillator (1 kHz) and detector, and the measurement uncertainty of the bridge assembly translates into a temperature uncertainty $\cong \pm 0.2$ mK.

Samples for electrical resistivity measurements were prepared by wrapping a long section (3 m) of the wire on a substrate of copper (transverse sample) or alumina (longitudinal sample) with General Electric (G.E.) 7031 varnish. A capacitance thermometer was attached to the substrate with the varnish, and the thermometer leads were tempered to the substrate. The substrate, in turn, was bolted to the copper post. The copper wire was wrapped noninductively on the substrate such that for the “transverse” sample a coil was produced with the axis of the coil oriented parallel to the field. For the “longitudinal” sample, a long, thin alumina plate was wrapped such that the major faces of the plate were parallel to the field. Usual four-lead potentiometric measurements were used wherein the current was supplied by a battery supply and the voltage drops measured on a digital voltmeter.

Zero-field resistivity measurements on the two samples agree to within about $\pm 2\%$ [i.e., $\rho(4 \text{ K}) = 9.032 \pm 0.152 \text{ n}\Omega \text{ cm}$]. There is a correction to the resistivity due to electron scattering at the wire surface (Nordheim’s rule), but this correction applies mainly to very pure copper wires.⁵ An estimate of this correction for the wire here indicates that surface scattering contributes $\lesssim 10\%$. This correction was ignored.

The transverse and longitudinal resistivity samples were each measured at 2.5, 5.0, 7.5, 10.0, and 12.5 T, each at several temperatures between 3–15 K (note from the inset in Fig. 1 that the T dependence of the resistivity is small). However, our transverse coil was not purely transverse but did contain a small ($\sim 6\%$) longitudinal component; similarly for our longitudinal coil. The ratios of these two components can easily be determined from the dimensions of the sample, and a separa-

tion of the components made. The measured resistivities were interpolated to give values at 1-K temperature intervals so that this separation was done at the same temperature.

This separation of the purely transverse and longitudinal components based on the geometries of the coils assumes that the magnetoresistance is a well-behaved function of the angle between the field and the wire axis, which is unproven. However, in our case this is a necessary assumption, and the angle involved in these coils was $\leq \pm 3^\circ$ from the pure transverse or pure longitudinal case.

The resulting “pure” resistivities, transverse and longitudinal, are summarized in the Kohler plot of Fig. 1. The transverse magnetoresistive effect is considerably *larger* than the longitudinal effect, and this result is not affected by the geometric separation of the components discussed above. The transverse data yield a good Kohler plot, whereas there is a considerable deviation in the longitudinal Kohler plot at 2.5 T. Shown for comparison in Fig. 1 is the Kohler plot reported by Fickett⁵ from measurements of the transverse magnetoresistance of a large number of copper samples.

The thermal conductivity data were measured on samples consisting of wire bundles (24 wires for the transverse sample, 6 wires for the longitudinal sample). One end of the wire bundle was wrapped noninductively around a capacitance thermometer using G.E. 7031 varnish, and the other end of the bundle was indium-soldered to a copper pin mounted in the reservoir post. Two heaters were mounted on the wire bundle at locations between the thermometer and the reservoir as follows: A manganin heater ($\sim 300 \Omega$) was wrapped on one end of a small alumina plate in a bifilar fashion using the 7031 varnish, and the wire bundle was wrapped noninductively around the other end of the alumina plate and attached with the varnish. The separation of the heaters was chosen to give a favorable A/l ratio (2.03-cm separation for the longitudinal sample, 10.9 cm for the transverse sample). For mechanical stability the wire bundles were woven inside parallel glass capillary tubes, and these tubes, in turn, were mounted on the reservoir post with Teflon fixtures. The axes of the glass tubes were arranged perpendicular to the magnetic field for the transverse sample, parallel to the field for the longitudinal sample. Care was taken to avoid any contact between the glass capillary tubes and the thermometer or heaters. An estimate of the error introduced by the capillary tubes indicated that this error was negligible due to

the high thermal conductivity of the copper wire bundle. Care was also taken to arrange the transverse sample such that the longitudinal component was minimized (15%), and similarly for the longitudinal sample (4%).

The heater resistances were corrected for the (slight) temperature dependence of the manganin wire,¹² and the power dissipated in the hookup leads was taken into account.¹³ The advantage of the "two-heater, one-thermometer" method for measuring thermal conductivity is that only *one* thermometer calibration is involved so that the ΔT 's can be measured very accurately ($\lesssim \pm 5$ mK). In this method the two heaters are separately activated to the same power level and ΔT is measured. The heater currents were measured by monitoring the voltage drop across a series resistor, and the capacitance thermometer was measured as mentioned above. $\Delta T/T$ values were maintained at 3–5%.

The zero-field thermal conductivities measured on the two samples are shown in Figs. 2 and 3, and there is good agreement between the two zero-field data sets (spread $\lesssim \pm 5\%$). The largest uncertainty in K results from determining the spacing of the two heaters.

The two data sets were separated into *pure* transverse and longitudinal components using the sample geometries, as was done above for the electrical resistivity data. To accomplish this, the $K(T)$ data

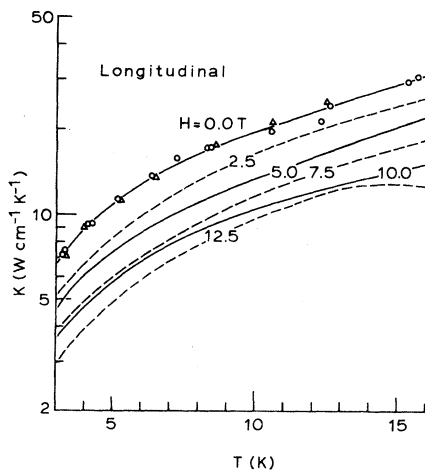


FIG. 3. Longitudinal magnetothermal conductivity data (see Fig. 2). The dashed curves at 2.5, 7.5, and 12.5 T were obtained using Eq. (1) and the longitudinal electrical resistivity data (see text).

sets were first fitted to a third-order expansion to determine the K 's at 1-K intervals. This expansion fitted the experimental data very well, as may be seen by the curve through the zero-field data in Figs. 2 and 3. In carrying out this separation of components, it is more convenient to deal with thermal resistances, which are additive, than with thermal conductances.

However, the transverse sample was measured at 2.5, 5, 7.5, 10, and 12.5 T whereas the longitudinal sample was only measured at 5 and 10 T (due to restrictions on magnet time). Consequently, an *exact* separation of thermal conductivity components could be done only at 5 and 10 T.

In order to determine transverse and longitudinal components at fields other than 5 and 10 T, the following procedure was used: The Lorentz numbers obtained from Eq. (1), based on the pure, transverse, and longitudinal electrical resistivities, and thermal conductivities at 0, 5, and 10 T, are shown plotted in Fig. 4 between 5–12 K. This temperature range was selected because above about 12 K the Wiedemann-Franz law is not strictly valid (see inset, Fig. 1), whereas below about 5 K it was believed that the multiple curve-fitting errors were unduly influencing the K/ρ ratio in Eq. (1). Moreover, as seen in Fig. 4, it is in this 5–12 range that the *zero-field* Lorentz numbers are in

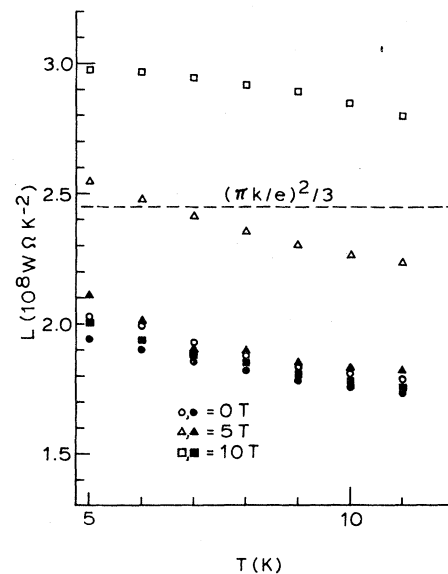


FIG. 4. Lorentz-number data at 0, 5, and 10 T obtained from experimental data. The open symbols are transverse data, the closed symbols, longitudinal data. The dashed line is the theoretical value of the Lorentz number.

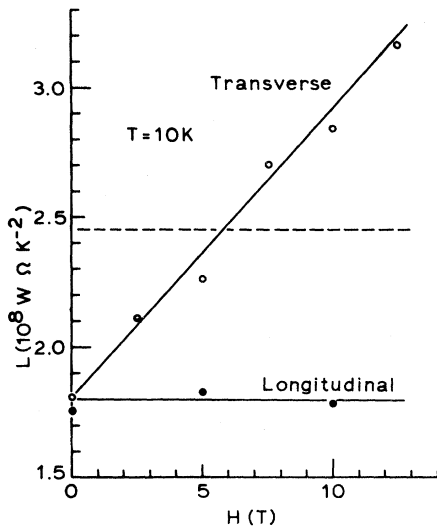


FIG. 5. H -field dependence of the transverse and longitudinal Lorentz numbers derived from the data in Figs. 1–4. The transverse Lorentz number varies linearly with H , $dL/dH = 0.112 \times 10^{-8} \text{ W } \Omega \text{ K}^{-2} \text{ T}^{-1}$. The dashed line is the theoretical value of the Lorentz number.

good agreement ($\sim \pm 1\%$).

From Fig. 4, the *transverse* Lorentz numbers have a significant H -field dependence, but the *longitudinal* Lorentz numbers are essentially H -field independent (the spread in the latter is $\lesssim \pm 2\%$). Therefore, assuming from Fig. 4 that the longitudinal Lorentz number is H -field independent, the longitudinal thermal conductivity can be determined directly from Eq. (1) from the longitudinal electrical resistivity data at 2.5, 7.5, and 12.5 T. These data are shown by the dashed curves in Fig. 3. And finally, these latter deduced data are used to separate the transverse component from the measured thermal conductivity data on the transverse sample at 2.5, 7.5, and 12.5 T, and these data are shown in Fig. 2. The transverse data in Fig. 2 at 2.5, 7.5, and 12.5 T are more reliable than the corresponding longitudinal data in Fig. 3 because the longitudinal component in the transverse sample was small (15%).

We finally arrive at the anisotropic H -field dependence of the Lorentz number from the above data and Eq. (1). This is shown in Fig. 5 for $T = 10 \text{ K}$ (similar plots are obtained at other temperatures, 5–12 K). The longitudinal Lorentz number is H -field independent, but the transverse Lorentz number varies linearly with field, $dL/dH = 0.112 \times 10^{-8} \text{ W } \Omega \text{ K}^{-2} \text{ T}^{-1}$ (on a relative basis, $\cong 5\%$ per tesla). This is a significant

H -field dependence as it implies that at $\cong 16 \text{ T}$ the transverse Lorentz number is doubled.

DISCUSSION

The literature on magnetoresistance phenomena in copper is quite extensive because high-field magnetoresistance data (and Hall-effect data) contain important information regarding the Fermi surface. The classic theoretical work on the Fermi surface of copper is Pippard's model.¹⁴ The vast majority of experimental studies have involved single crystals of copper of very high purity ($\text{RRR} > 20\,000$).

The longitudinal magnetoresistive data of Fig. 1 do not obey Kohler's rule at low-field levels. Anomalies have been reported in the longitudinal magnetoresistance of single crystals of copper,¹⁵ and these anomalies have been explained both in terms of the alignment sensitivity of the crystal to the field¹⁵ and in terms of the channeling of conduction electrons in a longitudinal field.¹⁶ It is interesting that the longitudinal magnetoresistance data of Fig. 1 do not display saturation with field, which for very pure copper single crystals limits $(\Delta\rho/\rho_0)_{\text{max}} \cong 0.98$.¹⁷ The explanation here may be the disproportionately large effect dislocations have on the longitudinal magnetoresistance.¹⁸ The data presented here demonstrate that both the electrical resistivity and the thermal conductivity of electrons in copper are more affected by a transverse field than a longitudinal field, as one would qualitatively expect from the way electrons spiral in a magnetic field.

We have no adequate explanation for the apparent linear dependence of the transverse Lorentz number on field, Fig. 5, which means that the resistivity increases with field faster than the conductivity decreases. In a longitudinal field, however, the two effects appear to exactly compensate. An explanation of these findings would entail a careful averaging over randomly oriented grains together with considerations of changes in the Fermi surface with temperature and intense magnetic fields.

Finally, the results presented here are of importance to the design of cryogenic devices where often the distinction between transverse and longitudinal magnetic field effects is not drawn. Also, the Wiedemann-Franz law is often invoked to estimate thermal conductivities from electrical resistivity data for commercial coppers,¹⁹ whereas the Fig. 5 data indicate that this procedure could seriously underestimate the thermal conductivity.

ACKNOWLEDGMENTS

The authors are grateful to the Purdue Materials Research Laboratory for use of the 14-T superconducting magnet facility and to the Francis Bitter

National Magnet Laboratory. Helpful discussions with Dr. R. R. Fickett are also gratefully acknowledged. This work was supported by the U. S. Air Force.

-
- ¹A. Wiedemann and W. Franz, *Ann. Phys. (Leipzig)* **89**, 497 (1853).
²N. F. Mott and H. Jones, *Theory of the Properties of Metals and Alloys* (Clarendon, Oxford, 1936).
³W. Hume-Rothery, *Atomic Theory for Students of Metallurgy* (Institute of Metals, London, 1955).
⁴M. Kohler, *Ann Phys. (Leipzig)* **5**, 99 (1949).
⁵See the review for copper by F. R. Fickett, International Copper Research Association Project No. 186 (Natl. Bur. Stand., Boulder, 1972).
⁶J. E. Huffman, M. L. Snodgrass, and F. J. Blatt, *Phys. Rev. B* **23**, 483 (1981), and references therein.
⁷W. N. Lawless, C. F. Clark, and R. W. Arenz, *Rev. Sci. Instrum.* (in press).
⁸H. M. Rosenberg, *Low Temperature Solid State Physics* (Clarendon, Oxford, 1963), Chap. 5.
⁹W. N. Lawless, *Rev. Sci. Instrum.* **42**, 561 (1971).
¹⁰W. N. Lawless, *Rev. Sci. Instrum.* **46**, 625 (1975).
¹¹W. N. Lawless and E. A. Panchyk, *Cryogenics* **12**, 196 (1972).
¹²W. N. Lawless, *Phys. Rev. B* **14**, 134 (1976).
¹³J. E. Neighbor, *Rev. Sci. Instrum.* **37**, 496 (1966).
¹⁴A. B. Pippard, *Philos. Trans. R. Soc. London Ser. A* **250**, 325 (1957).
¹⁵F. R. Fickett and A. F. Clark, *J. Appl. Phys.* **42**, 217 (1971).
¹⁶W. A. Reed, E. I. Blount, J. A. Marcus, and A. J. Arko, *J. Appl. Phys.* **42**, 5453 (1971).
¹⁷A. F. Clark and R. L. Powell, *Phys. Rev. Lett.* **21**, 802 (1968).
¹⁸P. G. Klemens and J. L. Jackson, *Physica* **31**, 1421 (1965).
¹⁹W. Nick and C. Schmidt, *IEEE Trans. Magn.* **17**, 217 (1981).